Worcester Polytechnic Institute
Digital WPI

Mechanical Engineering Faculty Publications | Department of Mechanical Engineering

8-1-2008

Lotka-Volterra Systems in Environments with Randomly Disordered Temporal Periodicity

Arvid Naess

Mikhail F. Dimentberg
Worcester Polytechnic Institute, diment@wpi.edu

Oleg Gaidai

Follow this and additional works at: https://digitalcommons.wpi.edu/mechanicalengineering-pubs

 Part of the Mechanical Engineering Commons

Suggested Citation

Naess, Arvid , Dimentberg, Mikhail F. , Gaidai, Oleg (2008). Lotka-Volterra Systems in Environments with Randomly Disordered Temporal Periodicity. *Physical Review E, 78*(2).
Retrieved from: https://digitalcommons.wpi.edu/mechanicalengineering-pubs/22

This Article is brought to you for free and open access by the Department of Mechanical Engineering at Digital WPI. It has been accepted for inclusion in Mechanical Engineering Faculty Publications by an authorized administrator of Digital WPI. For more information, please contact digitalwpi@wpi.edu.

Lotka-Volterra systems in environments with randomly disordered temporal periodicity

Arvid Naess*
Department of Mathematical Sciences, NTNU, NO-7491 Trondheim, Norway

Michael F. Dimentberg†
Mechanical Engineering Department, Worcester Polytechnic Institute, Worcester, Massachusetts 01609, USA

Oleg Gaidai‡
Centre for Ships and Ocean Structures, NTNU, NO-7491 Trondheim, Norway

(Received 21 November 2007; revised manuscript received 27 March 2008; published 20 August 2008)

A generalized Lotka-Volterra model for a pair of interacting populations of predators and prey is studied. The model accounts for the prey's interspecies competition and therefore is asymptotically stable, whereas its oscillatory behavior is induced by temporal variations in environmental conditions simulated by those in the prey's reproduction rate. Two models of the variations are considered, each of them combining randomness with "hidden" periodicity. The stationary joint probability density function (PDF) of the number of predators and prey is calculated numerically by the path integration (PI) method based on the use of characteristic functions and the fast Fourier transform. The numerical results match those for the asymptotic case of white-noise variations for which an analytical solution is available. Several examples are studied, with calculations of important characteristics of oscillations, for example the expected rate of up-crossings given the level of the predator number. The calculated PDFs may be of predominantly random (unimodal) or predominantly periodic nature (bimodal). Thus, the PI method has been demonstrated to be a powerful tool for studies of the dynamics of predator-prey pairs. The method captures the random oscillations as observed in nature, taking into account potential periodicity in the environmental conditions.

DOI: 10.1103/PhysRevE.78.021126 PACS number(s): 02.50.−r, 87.23.Cc

I. INTRODUCTION

In this paper we shall consider a generalized Lotka-Volterra (LV) model as governed by the following pair of differential equations:

$$\dot{U} = -mU + k\beta UV,$$

$$\dot{V} = \alpha V[1 + h(t)] - \beta UV - \gamma V^2. \tag{1}$$

As far as application to population dynamics is concerned, which is seemingly the most important field of application at present, the model (1) describes oscillatory behavior of the population sizes of two nonlinearly interacting species (the predator-prey or parasite-host pairs) [1–6]. In this case $U(t)$ and $V(t)$ are the population sizes of the predators (or parasites) and prey (or hosts), respectively, whereas the function $h(t)$ simulates the influence of temporal variations in the environmental conditions through those of the prey's reproduction rate α. The term with V^2 governs self-limitation in the growth of the prey population size in the absence of predators; it should be taken into account whenever $h(t)$ may contain random component(s) [1,2]. Indeed, population abundances as observed in nature are mostly of a random nature. They may be nice narrowband processes as shown in Fig. 1, which is similar to an illustration in [7], both being based on data from [8,9]. Or they may be highly intermittent processes with rare relatively short high-level outbreaks and almost zero levels between the outbreaks, like populations of budworms (forest parasites) as described in [10]. An extensive review of population dynamics of voles and lemmings in the face of random influences is given in [11].

Thus, the straightforward approach to simulation of phenomena of this kind would be analysis of Eqs. (1) with $h(t)$ being regarded as a random process with given properties. The analysis may be used, in particular, to predict the probability for quasiextinction [12] through solution of the so-called first-passage problem for the corresponding stochastic differential equations (SDEs) (1). The simplest model of this kind is a zero-mean "physical" Gaussian white noise $h(t)$ (in the Stratonovich sense) [1,2], so that

$$h(t) = \xi(t), \tag{2}$$

where $\langle \xi(t) \rangle = 0$ and $\langle \xi(t)\xi(t+\tau) \rangle = D_\xi \delta(\tau)$, where angular brackets denote probabilistic averaging, D_ξ is a positive constant, and $\delta(\cdot)$ is the Dirac delta function. The system (1) and (2) may be studied using the theory of Markov processes, which leads to the Fokker-Planck-Kolmogorov (FPK) partial differential equation for the joint probability density function (PDF) of the system's state variables [1,2,13,14]. An analytical solution to the specific FPK equation for the stationary joint PDF $p_{UV}(u,v)$ of $U(t)$ and $V(t)$ corresponding to the system (1) and (2) has been derived in [13] and studied in [13,15]. These results will be briefly outlined in Sec. II to be used as benchmarks for subsequent numerical studies. Furthermore, the expected time to quasiextinction has been

*Also at Centre for Ships and Ocean Structures, NTNU, Trondheim, Norway. arvidn@math.ntnu.no
†diment@wpi.edu
‡oleg.gaidai@ntnu.no

 ©2008 The American Physical Society

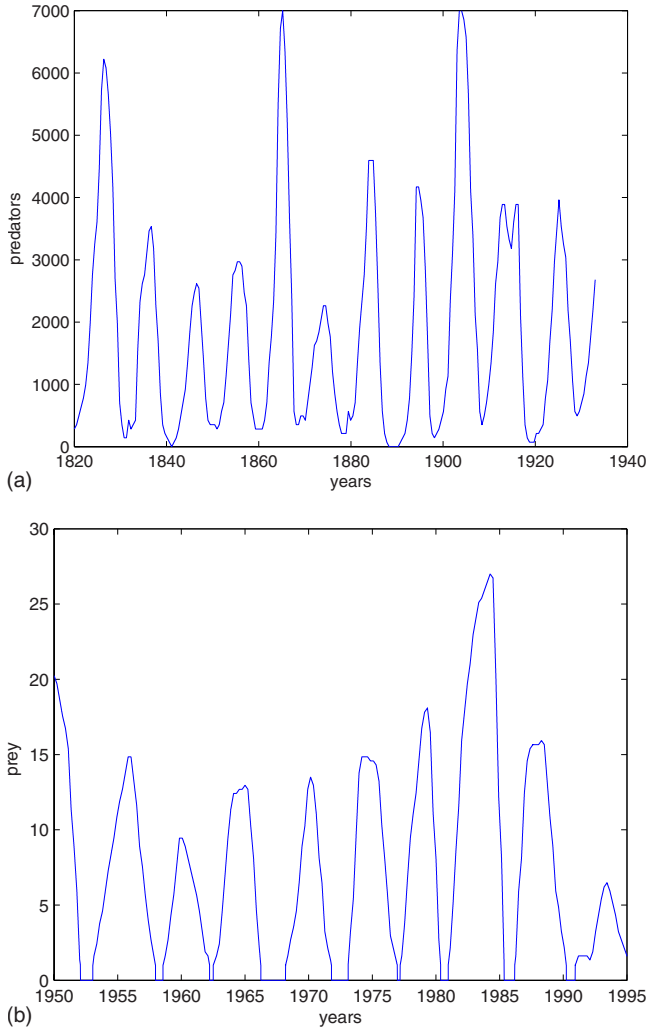

FIG. 1. (Color online) Historical time series of (a) predators (Canadian lynx) and (b) prey (gray-sided vole). Based on data from [8,9].

found in [13] using an asymptotic method of quasiconservative averaging to solve the relevant partial differential equation of the theory of Markov processes.

The above model (1) and (2) and the resulting solution to the corresponding FPK equation [13,15] seem to be adequate for simulating dynamics in a large variety of predator-prey pairs. However, the purely random model (2) does not account for potential periodicity in $h(t)$, for example due to annual seasonal variations in the environmental conditions, which may be important for some applications. Thus, the case of purely periodic (sinusoidal) $h(t)$ has been considered in [7], including specific examples of subharmonic resonances of various orders. However, the model of perfectly periodic environmental variations cannot completely explain the random nature of the observed oscillations. It may be argued, of course, that in some cases the sinusoidal variations may lead to chaos, so that the observed oscillations may be regarded as being chaotic rather than random. While the present authors agree with this point of view, it should be emphasized that generation of chaos by sinusoidal excitation may be quite sensitive to any imperfections in periodicity as was demonstrated in [16] for a (strongly nonlinear) single-degree-of-freedom system with impacts (chaos with "breeding of response frequencies" could be completely killed by random white-noise variations in the phase of the excitation as described by the model (4) to follow).

Thus, it seems appropriate to study the system (1) for a random $h(t)$ with some "hidden" periodicity, or for a periodic $h(t)$ with some random disorder. Two such models of $h(t)$ are adopted in this paper. The first one, which is used in Sec. IV, implies just simple addition of a zero-mean Gaussian white noise $\xi(t)$ [cf. Eq. (2)], to the sinusoid, i.e.,

$$h(t) = \lambda \sin \nu t + \xi(t). \tag{3}$$

The other model, which is used in Sec. V, implies random white-noise temporal variations in the phase of the sinusoid [13,14], i.e.,

$$h(t) = \lambda \sin Z(t),$$

$$\dot{Z} = \nu + \xi(t), \tag{4}$$

where $\xi(t)$ is the same as above.

The random process (4) has a continuous power spectral density (PSD) $\Phi_{hh}(\omega)$ [14],

$$2\pi\Phi_{hh}(\omega) = \frac{\lambda^2 D_\xi}{2} \frac{\omega^2 + \nu^2 + D_\xi^2/4}{(\nu^2 + D_\xi^2/4 - \omega^2)^2 + \omega^2 D_\xi^2}, \tag{5}$$

whereas its PDF is strongly non-Gaussian and bimodal, being nonzero only within $(-\lambda, +\lambda)$, with (integrable) singularities at $h=-\lambda$ and $+\lambda$. This process is seen to be narrow-band if $D_\xi/2 \ll \nu$, with ν and $D_\xi/2$ being, respectively, the mean frequency and bandwidth of $h(t)$. With increasing bandwidth, the peak frequency ω_* of $h(t)$ is reduced according to the relation $\omega_*^2 = \nu^2[-(1+D_\xi^2/4\nu^2)+2\sqrt{1+D_\xi^2/4\nu^2}]$ so that $h(t)$ may be regarded as being broadband whenever D_ξ and ν are of the same order.

Thus, each of the models (3) and (4) for $h(t)$ accounts for both randomness and periodicity as brought by the environment into the LV system (1). A numerical study of the corresponding system's steady-state response is presented in Secs. IV and V. The main tool for the numerical analysis is described in Sec. III; it is the path integration (PI) method which provides the stationary joint PDF of the responses.

II. BENCHMARK ANALYTICAL RESULTS

The logarithmic transformation

$$X = \ln U, \quad Y = \ln V \tag{6}$$

reduces Eqs. (1) to the form

$$\dot{X} = -m + k\beta \exp Y = \frac{\partial H}{\partial Y},$$

$$\dot{Y} = \alpha - \beta \exp X - \gamma \exp Y = -\frac{\partial H}{\partial X} - \frac{\gamma}{k\beta}\frac{\partial H}{\partial Y} + \alpha h(t), \tag{7}$$

where

$$H(X,Y) = k\beta \exp Y - mY + \beta \exp X - (\alpha - \gamma m/k\beta)X. \quad (8)$$

It is assumed in this section that $h(t)=\xi(t)$ (the common chain rule for differentiation may still be used for a "physical" white noise). Then the joint PDF $p_{XY}(x,y)$ of the transformed random state variables $X(t)$, $Y(t)$ satisfies the well-known FPK equation [1,2,13,15] which has the following exact stationary (independent of time) solution [13,15]:

$$p_{XY}(x,y) = C \exp[-(2\gamma/k\beta D_\xi \alpha^2)H(x,y)]. \quad (9)$$

Here C is a constant determined by the normalization condition.

Returning in Eq. (9) to the original state variables U,V and imposing the normalization condition within the first quadrant of the (u,v) plane yields the joint stationary PDF $p_{UV}(u,v)$ of the population sizes as a product of the individual one-dimensional PDFs of U and V [13,15]:

$$p_{UV}(u,v) = p_U(u)p_V(v),$$

$$p_U(u) = [(\delta/k)(\delta u/k)^{(\delta u_0/k)-1} \exp(-\delta u/k)]/\Gamma(\delta u_0/k),$$

$$p_V(v) = [\delta(\delta v)^{\delta v_0 - 1} \exp(-\delta v)]/\Gamma(\delta v_0), \quad (10)$$

where

$$u_0 = (\alpha - \gamma m/k\beta)/\beta = (\alpha/\beta)(1 - v_0/v_*),$$

$$v_0 = m/k\beta, \quad v_* = \alpha/\gamma, \quad \delta = 2\gamma/D_\xi \alpha^2. \quad (11)$$

Here $\Gamma(\cdot)$ is the Euler Gamma function, whereas u_0 and v_0 are steady-state values of $U(t)$ and $V(t)$, respectively, in the absence of the environmental variations; that is, they correspond to zero right-hand sides of Eqs. (1) with $h(t)\equiv 0$. The equilibrium point (u_0,v_0) is asymptotically stable as long as $\gamma>0$. The solution (10) implies that both population sizes are independent Γ-distributed stationary random processes provided that $u_0>0$ or $v_0<v_*=\alpha/\gamma$. Otherwise, the PDF of $U(t)$ has a nonintegrable singularity at $u=0$, and thus degenerates into the Dirac δ function at zero; this is the case (not considered here) where the predators become extinct and the growth of the population of prey is limited by their interspecies competition.

The mean values and variances of $U(t)$ and $V(t)$ can be easily calculated as $m_u=u_0$, $m_v=v_0$, and $\sigma_u^2=u_0k/\delta$, $\sigma_v^2=v_0/\delta$, respectively, so that the ratios of standard deviations to the corresponding mean values are

$$\sigma_u/m_u = \sqrt{k/\delta u_0}, \quad \sigma_v/m_v = \sqrt{1/\delta v_0}. \quad (12)$$

The PDFs of $U(t)$ and $V(t)$ are seen to have sharp peaks at their mean values if D_ξ is sufficiently small. On the other hand, if $\delta v_0<1$ $(\delta u_0/k<1)$, then $p_V(v)$ $[p_U(u)]$ has an integrable singularity at $v=0$ $(u=0)$.

Two other useful functionals of the joint response PDF (besides first- and second-order moments) may also be considered. First, the ratio of stay times above and below the mean level, say, for the parasites, may be predicted as the ratio of the corresponding cumulative probabilities,

$$\lambda_u = \frac{\mathrm{Prob}(U>u_0)}{\mathrm{Prob}(U<u_0)} = \frac{\int_{u_0}^{\infty} p_U(u)du}{\int_0^{u_0} p_U(u)du}$$

$$= \frac{\Gamma(z_0,z_0)}{\Gamma(z_0)-\Gamma(z_0,z_0)} = \lambda_x = \frac{\int_{x_0}^{\infty} p_X(x)dx}{\int_{-\infty}^{x_0} p_X(x)dx}, \quad (13)$$

where $z_0=\delta u_0/k$ and $x_0=\ln u_0$. The function $\Gamma(\cdot,\cdot)$, which depends on two arguments, is the incomplete Gamma function. A similar ratio may be calculated for the prey, using the last expression (13) with $z_0=\delta v_0$ instead of $z_0=\delta u_0/k$. Asymptotic expressions for the complete and incomplete Gamma functions indicate that this ratio approaches zero with $z_0\to 0$, and approaches unity with $z_0\to\infty$. The lower equality in Eq. (13) is obvious as long as the events $U>u_0$ and $X>x_0=\ln u_0$ are equivalent. It will be used to predict the ratio of stay times for predators from the numerically generated joint PDF of $X(t)$ and $Y(t)$ for general cases of the system (1) where the analytical solution (9) is not valid. A similar ratio for the prey can be calculated in the same way as long as $\lambda_v=\lambda_y$.

Second, the expected number $n_U^+(u)$ of up-crossings per unit time of a given arbitrary level u by $U(t)$ can be calculated as

$$n_U^+(u) = \int_0^\infty \dot{u} p_{U\dot{U}}(u,\dot{u})d\dot{u} = \int_{v_0}^\infty k\beta u(v-v_0)p_{UV}(u,v)dv$$

$$= n_X^+(x) = \int_{\ln(m/k\beta)}^\infty [k\beta \exp(y) - m]p_{XY}(x,y)dy. \quad (14)$$

The last expression in Eq. (14) may be used for the general case of system (1) where the analytical solution (9) is not valid and the numerically generated joint PDF of $X(t),Y(t)$ should be relied upon. For the special case when Eq. (10) is a valid substitution, it is obtained that

$$n_U^+(u) = (k\beta/\delta)(\delta v_0)^{\delta v_0}(\delta u/k)^{\delta u_0/k} \exp(-\delta v_0 - \delta u/k)$$
$$\times[\Gamma(\delta v_0)\Gamma(\delta u_0/k)]^{-1}. \quad (15)$$

The last formula provides just the expected frequency of oscillations if up-crossings of the mean or expected level $(u=u_0)$ are considered:

$$n_U^+(u_0) = n_\infty f(\delta v_0) f(\delta u_0/k), \quad (16)$$

where

$$n_\infty = \lim_{\delta\to\infty} n_U^+(u_0) = \Omega/2\pi, \quad \Omega = \beta(ku_0v_0)^{1/2},$$

$$f(z) = (2\pi)^{1/2} z^{z-1/2} \exp(-z)/\Gamma(z). \quad (17)$$

The quantity Ω can be clearly identified as the system's natural frequency of oscillations with small deviations of $U(t)$ and $V(t)$ from their steady values. Indeed, Eqs. (1) linearized in the vicinity of the equilibrium point u_0,v_0 can be reduced to the following linear second-order ordinary differential equation

$$\ddot{V}' + \gamma v_0 \dot{V}' + \Omega^2 V' = \alpha v_0 h(t), \tag{18}$$

where $V' = V - v_0$, which also shows the half-power bandwidth of the linearized system to be $\gamma v_0/2 = \gamma m/2k\beta$.

Applying Eq. (15) with the numerically generated joint PDF $p_{XY}(x,y)$ for the special value $x = x_0 = \ln u_0$ results in the expected circular frequency of oscillations. The ratio of the latter to $\Omega/2\pi$—the limiting value of $n_U^+(u_0) = n_X^+(x_0)$ for small-amplitude response—indicates the general level of nonlinearity involved in the numerically predicted response. In general, Eq. (14) may be used for large deviations of x from x_0 which may be of importance for estimating the probability of quasiextinction.

The above analytical results have been used in [15] to study the phenomenon of intermittency whereby rare and violent outbreaks in the response alternate with long periods of almost zero response level. It was shown that $U(t)$ and/or $V(t)$ should be of such nature if $\delta u_0/k \ll 1$ and/or $\delta v_0 \ll 1$. These analytical results will be used here to derive "nonparametric" criteria for intermittency that can be applied to numerically generated response PDFs.

(1) As can be seen from the Eqs. (12), the process(es) $U(t)$ and/or $V(t)$ should be of intermittent nature whenever

$$\sigma_u \gg m_u = u_0 \quad \text{and/or} \quad \sigma_v \gg m_v = v_0. \tag{19}$$

(2) As can be seen from Eq. (13) and the similar expression for λ_v, the process(es) $U(t)$ and/or $V(t)$ should be of intermittent nature whenever

$$\lambda_u \ll 1 \quad \text{and/or} \quad \lambda_v \ll 1. \tag{20}$$

While these criteria on the indices look somewhat loose, they are not more loose than the definition of intermittency.

It may also be convenient to define two different types of intermittency: type I is due to a high level of variations in the environmental conditions (small δ due to large D_ξ) with both $U(t)$ and $V(t)$ being of intermittent nature; and type II is due to small u_0 whereby only the population of predators (parasites) is of an intermittent nature whenever it is close to extinction. It goes without saying that both mechanisms for intermittency may coexist for a given system.

In concluding this section, it should be stressed that the numerical study as described in the following will be applied to the transformed equations (7) and (8) for the transformed state variables $X(t)$ and $Y(t)$. This is important to avoid, or at least reduce, numerical problems due to potential singularities in the calculated PDFs.

III. THE PATH INTEGRATION METHOD

For a detailed description of the path integration method and important aspects of its implementation, we refer to [17,18]. In the present paper a recently developed path integration (PI) technique was used [19]. It incorporates cubic B-spline interpolation in combination with a fast Fourier transform (FFT) method. The latter significantly accelerates the code, since instead of iterative integration, multiplication of characteristic functions is done. The PI coding was done in FORTRAN. As a simple convergence criterion we chose to match the first few moments estimated from Monte Carlo simulations and from the PDF calculated by PI.

In more detail, let us consider the three-dimensional (3D) dynamic system, discretized with time step Δt and with the random excitation entering only in the third dimension,

$$X = X' + a_1(X', Y', Z')\Delta t,$$

$$Y = Y' + a_2(X', Y', Z')\Delta t,$$

$$Z = Z' + a_3(X', Y', Z')\Delta t + \sqrt{D_\xi}\Delta B(t), \tag{21}$$

where $\mathbf{Z} = (X, Y, Z)^T$ and $\mathbf{Z}' = (X', Y', Z')^T$ represent the state space vector at the present time instant t and at the previous time instant $t' = t - \Delta t$, respectively. $B(t)$ denotes a standard Brownian motion process, and $\Delta B(t) = B(t) - B(t')$. To solve the discretized SDE (21), the PI technique is used. It is based on the total probability law, which reads

$$p(\mathbf{z},t) = \int_{\mathbf{R}^n} p(\mathbf{z},t|\mathbf{z}',t')p(\mathbf{z}',t')d\mathbf{z}', \tag{22}$$

where $p(\mathbf{z},t)$ denotes the PDF of the state space vector $\mathbf{Z}$ at time t, and $p(\mathbf{z},t|\mathbf{z}',t')$ denotes the transition PDF of $\mathbf{Z}$ at time t given that $\mathbf{Z}' = \mathbf{z}'$ at time t'. This means that, for each point $\mathbf{z}$, the value of the probability density function at a time t can be calculated as an integral based on the previous PDF at time $t' = t - \Delta t$, if the path from $\mathbf{z}'$ to $\mathbf{z}$ can be calculated. Time can therefore be discretized with constant time steps Δt using a fourth-order Runge-Kutta scheme: $a_j(z')\Delta t \rightarrow r_j(z', \Delta t)$, $j = 1,2,3$. The integral (22) requires the (incremental) transition probability density. It follows from Eq. (21) that this is a degenerate multivariate Gaussian distribution which assumes the following form:

$$p(\mathbf{z},t|\mathbf{z}',t') = \delta(x - x' - r_1(\mathbf{z}',\Delta t))\,\delta(y - y' - r_2(\mathbf{z}',\Delta t)) \times \frac{1}{\sqrt{2\pi D_\xi \Delta t}} \exp\left(-\frac{[z - z' - r_3(\mathbf{z}',\Delta t)]^2}{2D_\xi \Delta t}\right). \tag{23}$$

Note that one needs to evaluate the PDF at time t' at values of the state space variable arguments that do not coincide with the initially chosen grid points. This is where the interpolation technique is required, which makes it possible to represent the PDF at all points in the requisite domain. It is shown in [19] that, by combining Eqs. (22) and (23) with a variable transformation, the integral can be reduced to a convolution, which makes it possible to use FFT techniques to obtain fast iterations of the integration process needed to produce the PI solution.

An advantage of the PI method, if it is properly implemented, is its ability to produce very accurate solutions. However, a main drawback is the limited number of dimensions it can handle. Currently, 4D problems can be solved at acceptable computational cost. Of course, an alternative numerical solution approach is always offered by the Monte Carlo simulation method. While this method is very attractive due to its versatility and simplicity, it cannot in practice provide information on the same level of detail as PI, par-

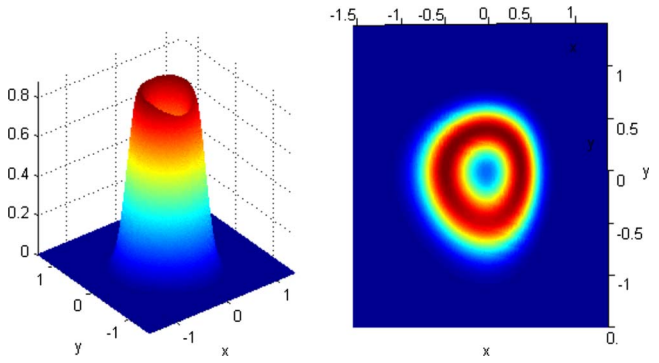

FIG. 2. (Color online) Time-averaged joint PDF by PI with contour plot on the right; $\lambda=0.05$, $x=\log_{10} u$, $y=\log_{10} v$.

ticularly for high deviations from mean values. Since our models in this paper are 2D and 3D, the PI is a very attractive method to use.

IV. THE CASE OF ADDITIVE RANDOM DISORDER

The system (3) and (7) is studied in this section. The numerical analysis is relatively simple since this is still the 2D case as long as the state variables $X(t)$ and $Y(t)$ are components of a two-dimensional Markov process. Indeed, simple addition of sinusoids does not bring any additional state variable(s). However it makes the response vector X,Y (periodically) nonstationary. Thus, the averaged-over-time joint PDF $p_{XY}(x,y)$ is presented in Figs. 2 and 3 as a 3D graph on the left together with its contour plot on the right. These results were obtained for the case $\alpha=1$, $m=1$, $k=1$, $\beta=1$, $\gamma=0.05$, $D_\xi=0.05$. These parameter values correspond to those in [7], which we shall subsequently call "Shaffer's case." The excitation frequency is $\omega=1$. The parameter λ is chosen to be 0.05 and 0.5.

V. THE CASE OF RANDOM PHASE DISORDER

The system (4) and (7) is studied in this section. The problem is now three dimensional when the 3D Markov process (X,Y,Z) is to be analyzed. The cases where the stationary process $h(t)$ with the PSD (5) is broadband and narrowband are considered in Secs. V A and V B, respectively. The

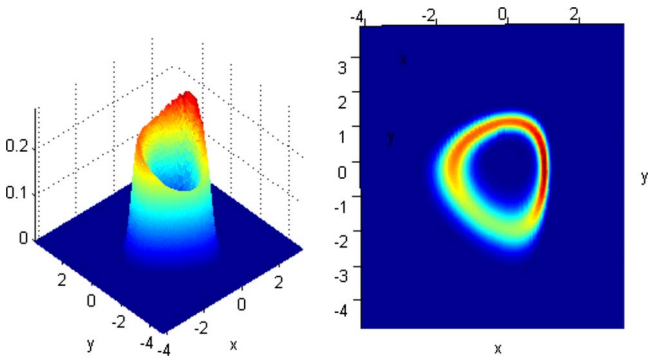

FIG. 3. (Color online) Time-averaged joint PDF by PI with contour plot on the right; $\lambda=0.5$, $x=\log_{10} u$, $y=\log_{10} v$.

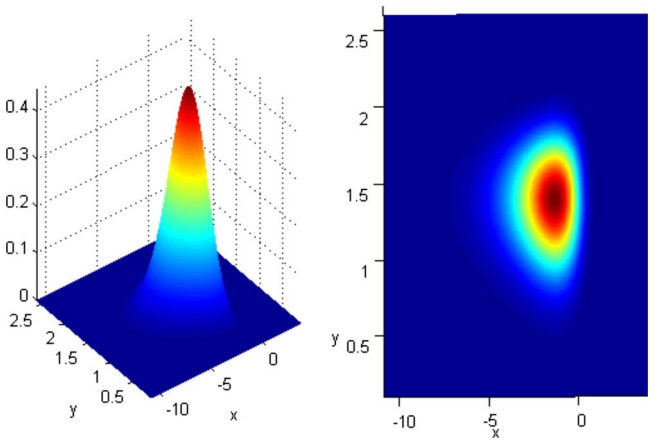

FIG. 4. (Color online) Asymptotic case: Joint PDF by PI with contour plot on the right; $x=\log_{10} u$, $y=\log_{10} v$.

former of these is studied, in particular, to test the numerical PI method with the analytical results. The latter case may very often be the more realistic. For example, one should not expect time shifts in such environmental temperature effects as "early spring" or "late autumn" to be larger than, say, one month; thus, standard deviations of annual phase variations should not exceed about 10% of the expected period of the variations (one year). Still, this kind of imperfect periodicity may exert a strong influence on the resulting dynamic response, particularly for highly resonant systems.

A. Broadband random variations

1. Asymptotic case

The following parameters are chosen: $\alpha=1/4$, $m=4$, $k=1$, $\beta=1$, $\gamma=10^{-4}$, $\lambda=0.03$, and $\nu=\Omega=1$. Choosing $\nu=\Omega$ gives the resonant case. The noise level is $D_\xi=1$. We may now compare these results with the analytical ones [13,15], relying on the Stratonovich-Khasminskii theorem [13,14]. The latter states that the response of a quasilinear system with natural frequency Ω to a stationary zero-mean broadband random excitation $h(t)$ approach asymptotically that of the averaged-over-period system to Gaussian white noise with intensity

$$D_\xi = 2\pi\Phi_{hh}(\Omega), \tag{24}$$

so that the actual PDF of $h(t)$ becomes "asymptotically irrelevant." It is true that the LV system (1) is not quasilinear in general, it may be just quasiconservative for vanishingly small γ and $h(t)$. However, in the case of a sufficiently small λ one may hope that the above statement is true as long as the system's response does not deviate much from its equilibrium state with natural frequency $\Omega=\beta\sqrt{ku_0v_0}$. Figure 4 presents the joint PDF $p_{XY}(x,y)$ and its contour plot obtained by PI.

The numerical solution by PI demonstrates very good matching with the analytical solution with $D_\xi=10^{-3}$; this intensity of the "equivalent" white noise having been calculated for the above system's parameters using formulas (5) and (24). The individual 1D PDFs of $X(t)$ and $Y(t)$ are prac-

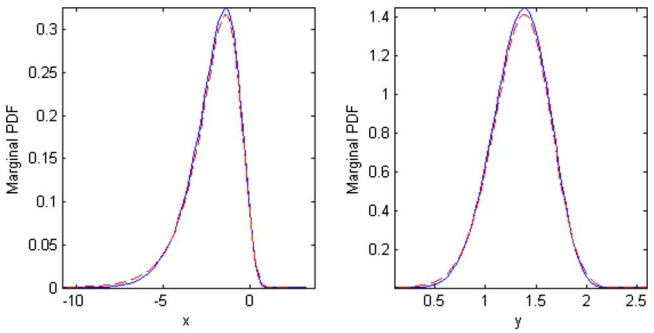

FIG. 5. (Color online) Asymptotic case: Comparison between PI (short dashed) and analytical (long dashed) 1D PDFs; $x=\log_{10} u$, $y=\log_{10} v$.

tically coincident with their analytical counterparts Eq. (10) as seen in Fig. 5. Furthermore, a numerical check indicated that the random variables X and Y are statistically independent, as they should be according to the analytical solution for the white-noise case (2). The expected upcrossing rate $n_U^+(u_0)$, $u_0=m_U$ was found to be $n_U^+(u_0)=0.144$ from PI, and $n_U^+(u_0)=0.143$ from the analytical solution Eq. (14). These values show that the oscillations are not perfectly linear, as expected since $2\pi n_U^+(u_0)/\Omega \cong 0.9<1$. This nonlinearity in response can also be clearly seen from lines of constant probability in Fig. 4, which are not perfectly elliptical as they should be in the case of small-amplitude lightly damped oscillations. Figure 5 compares PI with analytical 1D PDFs, and they are very close, as should be expected.

2. Intermittency case

Next we explore the case of intermittency, which is a phenomenon related to bifurcation mechanisms in nonlinear dynamical systems. For a discussion of the deterministic case, see [20]. For the particular case of the LV model, this is discussed in detail in [15]. Intermittency in the population of predators was observed in [15] under the following parameter values: $\alpha=1/4$, $m=4$, $k=1$, $\beta=1$, $\gamma=0.05$, $D_\xi=1$. In order to compare with the analytical solution, we use Eq. (24) to determine the following parameters $\lambda=1.1368$, $\nu=\Omega=0.447$. Figure 6 illustrates the numerically generated $p_{XY}(x,y)$. In the present case the parameters λ and γ are larger than in the previous example, while all other parameters are the same. These PI results are still found to be close to the analytical solution (9) with the corresponding $D_\xi=1.6$. For example, the value $n_U^+(u_0)=0.0345$ as found by the PI method is close to the analytical result $n_U^+(u_0)=0.0329$ from Eq. (14) ($u_0=m_U$). Thus, the expected period of the oscillations in the number of predators is about five times larger than the period $2\pi/\Omega$ of environmental variations. The analytical solution for this example with the "equivalent" $D_\xi=1.6$ indicates intermittency in the predators' population [15]. A similar effect should be expected in the present case according to the criteria (19) and (20) with values $m_u=0.05$, $\sigma_u=0.18$, and $\lambda_u=0.16$ obtained by the PI solution (this intermittency may be qualified as "mild" in the present case since inequalities of "much smaller type" are satisfied indeed, but not by an order of magnitude). Figure 7 illustrates samples of the processes $U(t)$ and $V(t)$ as obtained for this case by direct Monte Carlo simulation.

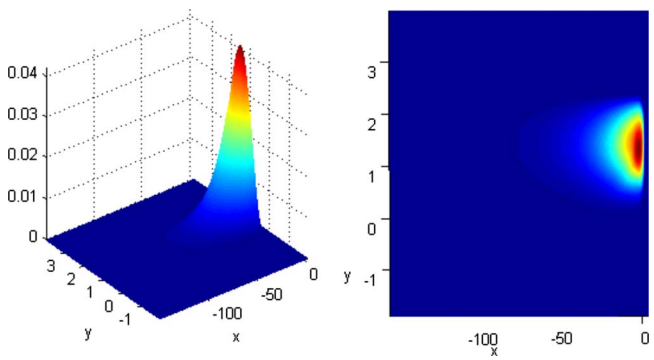

FIG. 6. (Color online) Intermittency case: Joint PDF by PI, contour plot at the right; $x=\log_{10} u$, $y=\log_{10} v$.

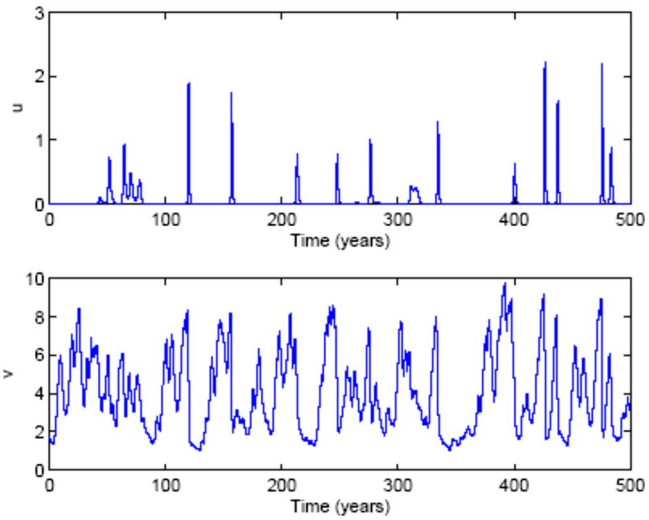

FIG. 7. (Color online) Intermittency case: Monte Carlo samples of $U(t)$ (predator) and $V(t)$ (prey).

Thus, the analytical solution for the LV system (1) for the white-noise case (2) may very often be used for approximate evaluation of some response characteristics in case of a broadband $h(t)$, although additional comparisons for nonresonant cases should also be made. However, it is the numerical solution by the PI method that should be relied upon whenever the tails of the response PDFs are sought for, e.g. for predicting excursion rates $n_U^+(u)$ at high levels.

It is interesting to note that for the case studied $n_U^+(u_0)$ is almost independent of the noise level D_ξ. The explanation lies in the nature of the noise, i.e., phase disorder. Moreover, when the noise level D_ξ is increased, for example up to 25, the match between the PI and analytical PDFs becomes perfect.

B. Narrowband random variations

In this section we consider once again the law (4) for $h(t)$, but for the narrowband case $\nu=1$ and $D_\xi=0.05$. The corresponding relative bandwidth $D_\xi/2\nu=0.025$ may indeed be more appropriate for simulating random variations in phase of annual variations in the prey reproduction rate as long as

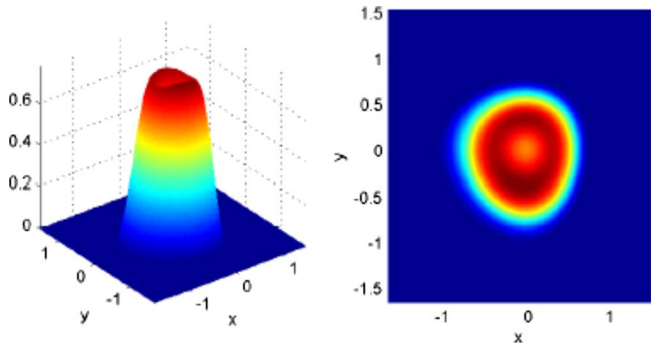

FIG. 8. (Color online) Joint PDF of stationary response; $\lambda=0.05$, $x=\log_{10} u$, $y=\log_{10} v$.

the latter is assumed to be proportional to environmental temperature. Thus, Figs. 8–10 illustrate the joint PDFs $p_{XY}(x,y)$ for $\alpha=1$, $m=1$, $k=1$, $\beta=1$, $\gamma=0.05$, $D_\xi=0.05$, $\nu=1\simeq\Omega$, and $\lambda=0.05,0.50,095$, respectively.

In the case of the smallest λ (Fig. 8), the oscillations are seen to be close to linear, with lines of constant probability being somewhat close to ellipses in this case where γ is also small. The PDF $p_{XY}(x,y)$ is seen to correspond to bimodal individual 1D PDFs of $X(t),Y(t)$. This finding correlates with the PI numerical solution [21] for a single-degree-of-freedom linear system under excitation of the form (4). That analysis highlighted the important nondimensional parameter as the excitation to system bandwidth ratio which is $R_B=D_\xi/\gamma v_0$ for the present linearized system (18). For $R_B\ll 1$ the response PDF was found to be close to that of a sinusoid with random phase and "smeared" singularities—thus definitely bimodal—whereas for $R_B\gg 1$ the PDF is indeed asymptotically Gaussian. A transition between unimodal and bimodal PDFs was found in [21] around $R_B=3.6$. It may be useful for interpreting numerical and observation data to adopt a convention whereby a system's response is qualified as being predominantly sinusoidal if its PDF is bimodal and predominantly random if it is unimodal.

With increasing λ the response level is increasing, as should be expected, and the response itself becomes "more nonlinear." This can be seen from lines of constant probability. The periodicity in response is still seen from the bimodality of the PDF of $Y(t)$.

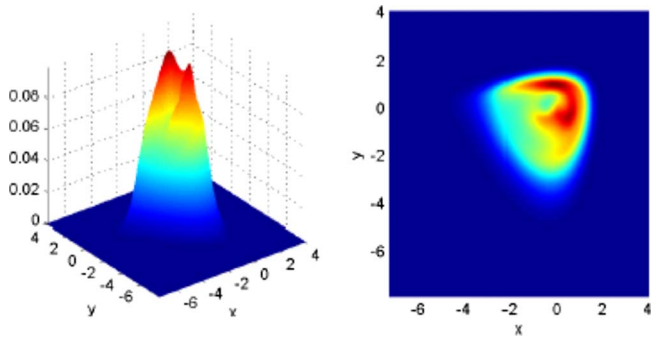

FIG. 9. (Color online) Joint PDF of stationary response; $\lambda=0.50$, $x=\log_{10} u$, $y=\log_{10} v$.

VI. COMMENTS AND CONCLUSIONS

The main goal of this paper was to apply the PI method for a study of the stochastic dynamics of Lotka-Volterra systems subjected to random temporal variations in the environmental conditions. While the latter were simulated just by variations in the prey's reproduction rate, the variations in the other system's parameter(s) may be similarly handled by the PI method as well. The laws considered for parameter variations combined hidden periodicity with randomness, thereby providing the possibility to account for the influence of, say, annual periodicity in the environmental conditions, which may be far from perfect in many applications. The joint PDFs of the population abundances as calculated by the PI method can be used for predicting important characteristics of the response—such as the expected number of crossings per unit time of a given level of the number of predators. Several specific examples considered in this paper demonstrate a certain qualitative difference in the predicted response PDFs for various cases. That is, in the case of a broadband random excitation (4) each of the two 1D individual PDFs of $X(t)$ and $Y(t)$ are found to be unimodal. Moreover, they are found to coincide with the analytically derived PDFs for the case where the analytical solution should be asymptotically applicable. On the other hand, the above PDFs may be bimodal in some cases of the narrowband random excitation. Thus, the responses with unimodal PDFs may be provisionally qualified as being predominantly random whereas those with bimodal PDFs are predominantly periodic. Applying this qualification rule to oscillations observed in nature, as presented in Fig. 1, we may qualify them as being predominantly random; see the estimated PDFs in Fig. 11 (peaks at the left sides are assumed to be within uncertainty limits).

Finally, it should be noted that the PI method may be similarly applied to another generalized version of the basic LV model (1). Actually the product-type nonlinearities represented by the terms $k\beta UV$ and βUV account just for the expected number of encounters of predators with prey as the main factor of their interaction. While this may very well be the case indeed, say, for parasite-host pairs, more complicated pursuit and evasion activity of the predators and prey during their encounters may be of importance in some cases. This can be accounted for by replacing the above interaction terms by $kUR(V)$ and $UR(V)$, respectively, where $R(V)$ is a

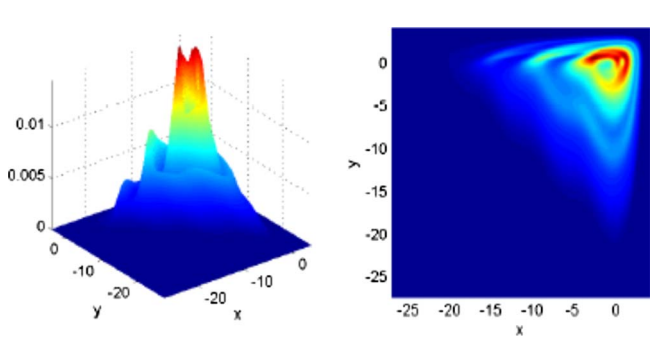

FIG. 10. (Color online) Joint PDF of stationary response; $\lambda=0.95$, $x=\log_{10} u$, $y=\log_{10} v$.

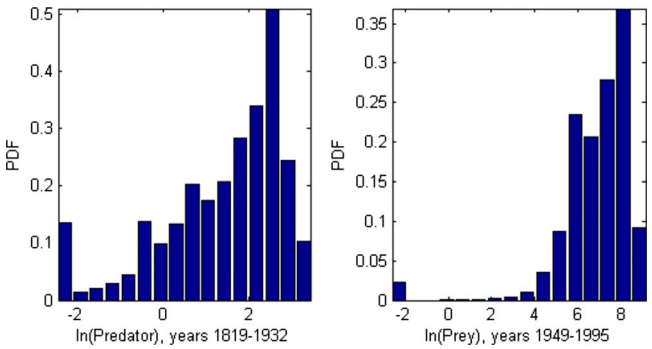

FIG. 11. (Color online) Estimated PDFs of the logged time series shown in Fig. 1. Left and right graphs correspond, respectively, to the populations of predators [Fig. 1(a)] and prey [Fig. 1(b)].

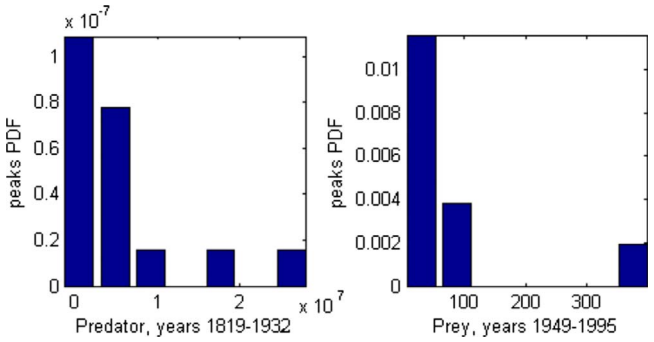

FIG. 12. (Color online) PDFs of peaks of the population number of predators as shown in Fig. 1(a) (left histogram) and of prey as shown in Fig. 1(b) (right histogram).

so-called functional response function which approaches a certain finite limit with $V \to \infty$ [2]. The corresponding deterministic generalized system, which has $h(t) \equiv 0$, has been analyzed in [2] for the case where the deviations of $R(V)$ from a linear function, as well as the coefficient γ, are proportional to a small parameter. The analysis was based on averaging over the closed-loop trajectories of the corresponding classical (conservative) LV system defined by Eqs. (1) with $h(t) \equiv 0$ and $\gamma = 0$. The analysis demonstrated the potential for existence of limit cycle(s) in the generalized LV systems under certain conditions imposed on $R(V)$. (If the extended LV system possesses a stable limit cycle it may be called "noisy clockwork;" indeed, the name was used in the title of a survey paper [22].)

An approximate analysis by quasiconservative stochastic averaging has been performed in [13,23] for the generalized LV system for the corresponding white-noise stochastic case (2). This resulted in a quadrature solution for the PDF of the "quasi-Hamiltonian" H as defined by Eq. (8). The solution can be used, in particular, to evaluate whether the observed oscillations are just forced by the parameter(s) variations or represent the limit-cycle oscillations as transformed by random excitation (case of noisy clockwork). The solution shows that the PDF of H has its peak at the system's equilibrium state in the former case, that is, at $H(x_0, y_0)$, and at a certain higher value of H in the latter case [23]. While this criterion for discrimination may not be especially convenient with H being unknown for the observed process $U(t)$ or $V(t)$, one may alternatively operate with *peaks* of the squared observed process. For example, for the process $U(t)$ illustrated as the upper trace in Fig. 1 (population of lynx) its mean value u_0 is calculated; then we calculate the process $\bar{U}^2 = [U(t) - u_0]^2$ and evaluate its peak values, which we denote as $\hat{S}$. The PDF $p_{\hat{S}}(s)$ should provide the same rule for discrimination between purely forced oscillations and noisy clockwork as long as $\hat{S}$ increases monotonically with H. This PDF for the time series in Fig. 1(a) is presented as the left histogram in Fig. 12. The conclusion seems to be that the case of purely forced oscillations is observed here, although it contains rather significant uncertainty due to the small sample available (11 peaks only). A similar conclusion can be made for the time series in Fig. 1(b)—see the histogram on the right in Fig. 12—although with even higher uncertainty (eight peaks only).

It goes without saying, of course, that the numerical PI method is not restricted by the above condition that the system should be asymptotically close to a conservative one. Furthermore, it can also be applied to other more sophisticated stochastic models of population dynamics including, for example, those with multiple stable equilibrium states as studied by direct numerical simulation in [24–26].

ACKNOWLEDGMENTS

This work was supported by the Research Council of Norway (NFR). The authors want to thank Dr. E. Mo from NTNU for his collaboration in path integration FORTRAN coding.

[1] R. M. May, *Stability and Complexity in Model Ecosystems* (Princeton University Press, Princeton, NJ, 1973).
[2] Ju. M. Svirejev and D. O. Logofet, *Stability of Biological Communities* (Nauka, Moscow, 1978) (in Russian).
[3] P. J. Wangersky, Annu. Rev. Ecol. Syst. **9**, 189 (1978).
[4] D. Ludwig, B. Walker, and C. S. Holling, Conserv. Ecol. **1**, 7 (1997).
[5] G. Q. Cai and Y. K. Lin, Sadhana: Proc., Indian Acad. Sci. **31**, 315 (2006).
[6] V. Křivan, Am. Nat. **170**, 771 (1997).
[7] W. M. Schaffer, B. S. Pederson, B. K. Moore, O. Skarpaas, A. A. King, and T. V. Bronnikova, Chaos, Solitons Fractals **12**, 251 (2001).
[8] C. S. Elton and M. Nicholson, J. Anim. Ecol. **11**, 215 (1982).
[9] T. F. Hansen, N. Chr. Stenseth, and H. Heltonen, Am. Nat. **154**, 129 (1999).
[10] T. Royama, *Analytical Population Dynamics* (Chapman & Hall, London, 1992).
[11] N. Chr. Stenseth, Oikos **87**, 427 (1999).
[12] L. R. Ginzburg, L. B. Slobodkin, K. Johnson, and A. G. Bind-

man, Risk Anal. **2**, 171 (1982).
[13] M. F. Dimentberg, *Statistical Dynamics of Nonlinear and Time-Varying Systems* (Research Studies Press, Taunton, U.K., 1988).
[14] Y. K. Lin and G. Q. Cai, *Probabilistic Structural Dynamics* (McGraw-Hill, New York, 1995).
[15] M. F. Dimentberg, Phys. Rev. E **65**, 036204, 2002.
[16] M. F. Dimentberg and D. V. Iourtchenko, Int. J. Bifurcation Chaos Appl. Sci. Eng. **15**, 2057 (2005).
[17] A. Naess and J. M. Johnsen, Probab. Eng. Mech. **8**, 91 (1993).
[18] A. Naess and V. Moe, Probab. Eng. Mech. **15**, 221 (2000).
[19] E. Mo and A. Naess, in *Proceedings of the Tenth International Conference on Applications of Statistics and Probability in Civil Engineering (ICASP10), Tokyo, 2007*, edited by J. Kanda, T. Takada, H. Furuta (Taylor and Francis, London, 2007).
[20] A. H. Nayfeh and B. Balachandran, *Applied Nonlinear Dyanmics* (John Wiley & Sons, New York, 1995).
[21] M. F. Dimentberg, E. Mo, and A. Naess, J. Eng. Mech. **133**, 1037 (2007).
[22] O. N. Bjornstad and B. T. Grenfeld, Science **293**, 638 (2001).
[23] M. F. Dimentberg, *Random Processes in Dynamic Systems with Variable Parameters* (Nauka, Moscow, 1989) (in Russian).
[24] A. B. Goryachev *et al.*, Chaos **6**, 78 (1996).
[25] B. E. Kendall, Chaos, Solitons Fractals **12**, 321 (2001).
[26] A. F. Rozenfeld *et al.*, Phys. Lett. A **280**, 45 (2001).